*University of*
HUDDERSFIELD

## University of Huddersfield Repository

Muller, Matthias and Barrans, Simon

Impact of flange geometry on the ultimate axial load capacity of V-band clamps

**Original Citation**

Muller, Matthias and Barrans, Simon (2010) Impact of flange geometry on the ultimate axial load capacity of V-band clamps. In: Conference papers: 9th International Conference on Turbochargers and Turbocharging. Institution of Mechanical Engineers, London, pp. 183-192. ISBN 978-1-907599-15-6

This version is available at http://eprints.hud.ac.uk/9784/

http://eprints.hud.ac.uk/

# Impact of flange geometry on the ultimate axial load capacity of V-band clamps

M. Muller, S.M. Barrans
School of Computing and Engineering, University of Huddersfield, UK.

**ABSTRACT**

Modern turbochargers typically comprise a body in three parts; the turbine and compressor housings and the bearing housing. The preferred method of joining these three parts, in automotive applications, is to use a band clamp with a flat bottomed V-shaped cross section mating with appropriate flanges on the body sections. This method of clamping allows for rapid assembly and infinitely variable relative rotational orientation of the body parts. In this paper finite element analyses are carried out to predict the influence of different flange geometries to the ultimate axial load capacity (UALC), which show a significant dependency on the flange thickness.

## 1    INTRODUCTION

V-band clamps are widely used in automotive, aircraft and aerospace industries to connect a pair of circular flanges to provide a joint with good axial strength and torsional rigidity. The band clamps this paper focuses on are mainly used to connect together housings of turbochargers for diesel engines. During the assembly process a V-band clamp is first loosely placed around the flanges, after that the T-bolt nut (Figure 1) is tightened. This leads to a radial force being generated in the band clamp, and, due to the V-section of the band this results in the creation of an axial load. This axial load then pushes the flanges together.
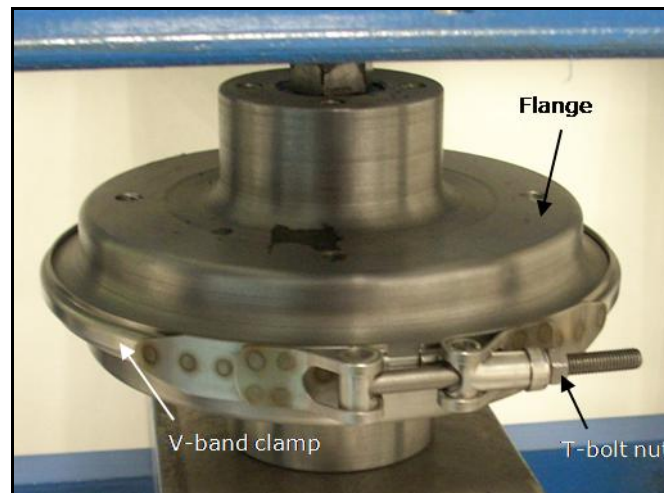


**Figure 1: V-band clamp assembled to a pair of circular test flanges [1]**

Several research papers by Shoghi et al. [2], [3] and [4] have been published concerning V-band clamps. In their work Shoghi et al. [2] present a classical analysis and Shoghi et al. [3] a finite element analysis to investigate stresses generated in the V-band during the assembly process. In Shoghi et al. [4] these results were backed up with experimental data and an updated method of determining the axial load generated by an assembled V-band clamp joint was presented.

Barrans and Muller [1] have recently developed an axisymmetric finite element model able to investigate the elastic-plastic material behaviour of V-band joints as the flanges are separated by an external force. This technique therefore allows the ultimate axial load capacity of V-band joints to be predicted. It should be noted that the work reported in [1] focused on setting up the model in the commercial FEA software ABAQUS and determining the appropriate settings for finite element parameters such as solver type, mesh density and especially the contact between the flanges and the band. The study was carried out with the V-band modelled as solid body using finite elements and the flange modelled using an analytical rigid body. It was found that an inappropriate mesh density or solver type would result in highly erroneous peak loads and hence potentially incorrect predictions of the UALC.

In this paper the influence of varying flange geometry to the ultimate axial load capacity of a V-band clamp joint has been investigated using the finite element model taken from Barrans and Muller [1]. The commercial finite element analysis package ABAQUS/Standard has been used to predict the UALC and model the differences in flange geometry.

## 2    FINITE ELEMENT MODEL

For the finite element models analysed in this paper a flange diameter of $D_f$= 235 mm was taken. This is a typical diameter for the V-band clamps that are used in turbocharger applications and it was shown by Barrans and Muller [1], that a maximum UALC appears to be at a flange diameter $D_f$ of 250 mm. 235 mm is the closest standard diameter value.

### 2.1    Set up of FE model
The finite element model [1] used for this simulation was assumed to be axisymmetric and the symmetry plane between two flanges made it possible to model only one side (see also Figure 2). Hence the model size could be reduced. The flange was modelled using an analytical rigid body since in many applications it will typically have a thickness many times greater than the thickness of the V-band and will therefore deform only slightly compared to the band. The use of a rigid body also dramatically reduced the analysis time. For the V-band clamp a solid body has been used. As the models include contact analyses, Dassault Systems [5] suggest the use of 2D plane strain linear elements with reduced integration for the V-band clamp, because second order elements suffer from a non uniform load distribution between mid-side and corner nodes. This element choice is also recommended by Konter [6]. Moreover unlike fully integrated linear elements, reduced integration linear elements do not suffer from shear locking which usually leads to under predicted results. The problem of hour-glassing often associated with reduced integration elements [7] is avoided by introducing a small amount of artificial "hourglass stiffness" and using a relatively fine mesh. A penalty contact algorithm was used as Konter [8] states that these tend to converge easily and also are more stable. An implicit solver was used to solve the analyses as suggested by Barrans and Muller [1], since that work showed that especially for this application, an implicit solver compared to their explicit counterparts tended to give more accurate results and need less CPU time.
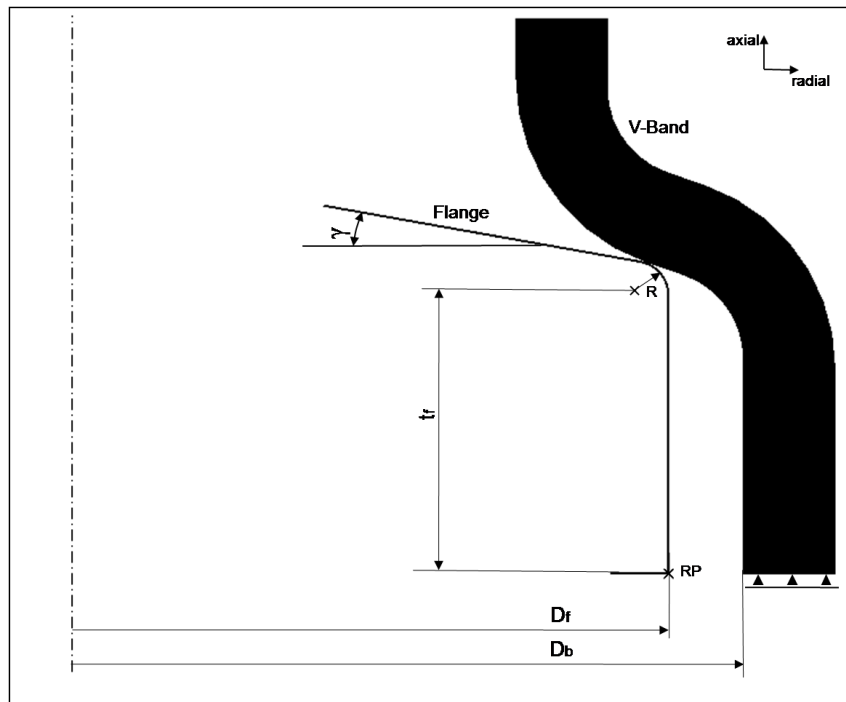


**Figure 2: Axisymmetric FE model showing all geometrical parameters**

In order to simulate the assembly process in which the T-bolt nut is tightened, an artificial thermal strain was generated in the band to shrink it onto the flanges. It was hereby assumed that deformation of the band and hence stresses are axisymmetric. The process of applying this thermal strain in ABAQUS/Standard is described in detail in section 2.4. A displacement boundary condition (BC) was applied at the reference point (RP in Figure 2) of the flange to prevent it from moving in the axial direction or rotating during assembly. The boundary condition needed to be applied only to the reference point as Dassault Systems [9] state that an analytical rigid body has two translational and one rotational degrees of freedom only at the reference point. As the flange is rigid, it needs to be constraint in theses three directions. A symmetry BC was applied at the symmetry plane of the V-band to prevent it from moving in the axial direction during the whole simulation. Being an analytical rigid body, the UALC can only be taken-up at the reference point RP of the flange.

### 2.2    Material Properties
AISI 304 stainless steel was used for the V-band clamp with a Young's Modulus of 227 GPa and a Poisson's Ratio of 0.29, which where taken from Shoghi [10]. In the FE analyses the material was assumed to be elastic-plastic with linear hardening, as described by Dixit and Dixit [11].

ABAQUS requires all material properties to be added as true stress, $\sigma_t$, and strain, $\varepsilon_t$, values so equations (1), (2) and (3) were used to convert the engineering values, $\sigma_e$ and $\varepsilon_e$, of the yield point and the ultimate tensile strength into true values, as demonstrated by Meyers and Chawla [12] and Teherani et al. [13].

$$\sigma_t = \sigma_e(1 + \varepsilon_e) \tag{1}$$

$$\varepsilon_t = \ln(1 + \varepsilon_e) \tag{2}$$

$$\varepsilon_{pl} = \varepsilon_t - \varepsilon_{el} \tag{3}$$

According to equations (1), (2) and (3) above, the true stress $\sigma_{ty}$ at the yield point was 648 MPa with no plastic strain, and the true stress $\sigma_{tUTS}$ at the ultimate tensile strength was 1182.7 MPa with a true strain $\varepsilon_t$ of 0.322 and a plastic strain $\varepsilon_{pl}$ of 0.317. All stress and strain properties discussed above can also be seen in the stress and strain diagram representing the material model in Figure 3. In there $\sigma_{tUTS}$ represents the true stress value of the ultimate tensile strength and $\sigma_{ty}$ represents the true stress value at the yield point.
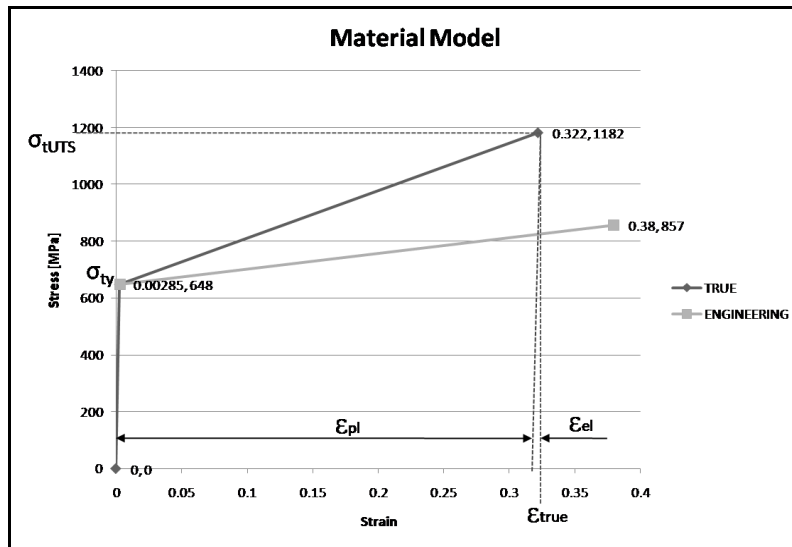


**Figure 3: Material model used for finite element analysis**

### 2.3   Flange geometry
The aim of this paper is to investigate how changes of the flange geometry affect the UALC. Therefore the three geometrical parameters of the flange angle, contact radius and thickness were chosen as variables. The flange angle, **γ**, usually is manufactured to fit the V-band clamp angle of 20°, [10], which was taken as the reference value. The whole range was from 18° to 22°, using steps of 1°. The contact radius R for turbocharger applications is normally 0.8 mm, as stated by Brown [14]. The range for R was from 0.6 mm to 1.0 mm. The reference value for the flange thickness $t_f$, as stated by Shoghi [10], was 4.5 mm with a tolerance of +2.5%. In this paper the range for tolerance was from -10% to +10%.

### 2.4   T-bolt load
As mentioned in section 2.1 the band clamp was shrunk onto the flange to simulate the process of tightening the T-bolt nut. The T-bolt induced load referred to in this paper is the axial load generated by the V-section pressing the flanges together as the nut is tightened. The value of this induced load in each analysis was measured using the axial reaction force at the reference point (RP) of the flange. An iterative process was required to determine the thermal load required to obtain the correct induced load for each analysis as due to the change of geometry, the contact point between flange and band clamp will change. If for example the thickness $t_f$ is reduced, the flange will be smaller, hence the contact point will move more towards the flat part of the V-band clamp, and therefore reducing the gap between flange diameter $D_f$ and band clamp diameter $D_b$ (also see Figure 2). The band will therefore have to be shrunk further to generate the required induced load. For all analyses the induced load was set to 6kN taken from Shoghi et al. [4].

### 2.5   Mesh
In the finite element analyses structured meshes were used because Barrans and Muller [1] showed that with structured meshes the contact analysis for this model is more stable and has fewer convergence problems than with free meshes. A relatively coarse mesh was used to model the V-band clamp. As initial finite element analyses have shown the mesh density does have a significant influence on the prediction of the plastic strain (PEEQ), as the coarse mesh under-predicts the plastic deformation at the initial contact point by about three times. However as this paper focuses on the overall deformation of the band section and not on deformations at the contact point, this highly localised plastic strain distribution can be ignored. A typical mesh density chosen for the finite element model can be seen in Figure 4 and Figure 5, both showing the undeformed case before the V-band clamp is assembled to the flanges, as well as the deformed case once full load is applied and

the joint has failed. Figure 4 also shows the equivalent plastic strain (PEEQ) and Figure 5 the von Mises stress for the fully loaded and deformed case. The thickness of elements on the inner surface of the band clamp is 0.082mm, which with a band clamp thickness of 1.2mm, gives a ratio of 0.068.

The values for UALC on the other hand differ only slightly with different mesh densities, e.g. for varying structured mesh densities the range for UALC was from 156 kN to 162 kN and for free meshes the range was 151 kN to 177 kN, considering that the element size at the contact area was the same for both kinds of meshes. Analyses using different mesh densities have shown that for a relatively coarse mesh compared to a fine mesh the UALC values only differ by a maximum of 2%. Moreover coarse mesh densities require less solver time.
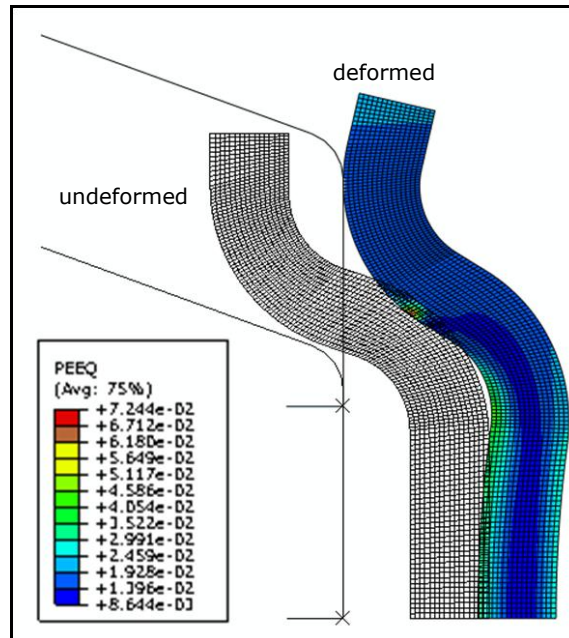


**Figure 4: FE model showing initial and deformed geometry and equivalent plastic strain PEEQ**
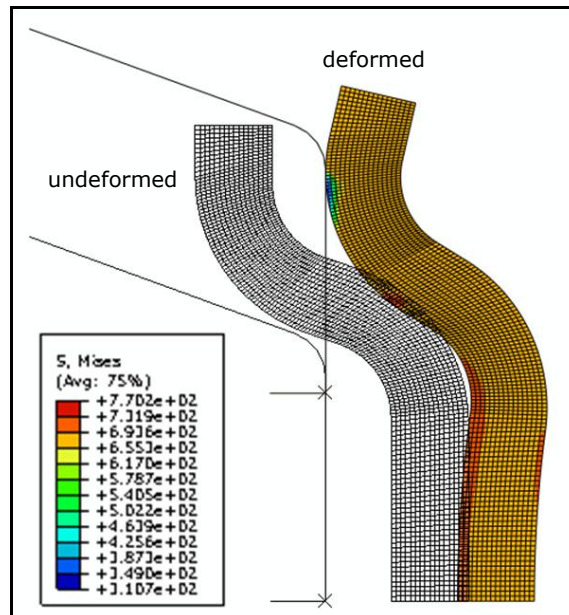


**Figure 5: FE model showing initial and deformed geometry and corresponding von Mises stress**

## 3    RESULTS

It can be seen in Figure 3 that the deformation of the V-band combines two modes. The first is an overall increase in the band diameter. The second is a bending of the V-band cross section. The presence of significant plastic strain only on the inner and outer surfaces of the band indicates that the bending mode is principally responsible for the stresses generated. However, it is clear that both deformation modes will have an impact on the UALC.

As the trend in Figure 6 shows, the UALC is highly dependent on the flange thickness $t_f$. It can be seen that the UALC drops as the flange gets thicker. Considering Figure 2 this is due to the flange contact point moving to the foot of the band section and hence increasing the lever responsible for bending the back of the section.
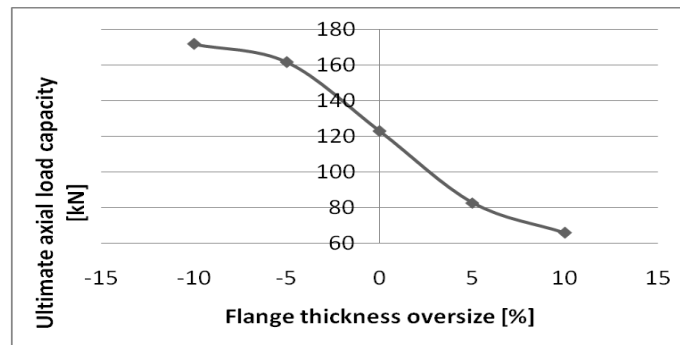


**Figure 6: Predicted UALC over the flange thickness oversize for a contact radius of 0.8mm and an angle of 20°**

Figure 7 shows the dependency of the UALC on the flange radius R. Although the influence of the radius is rather small compared to the flange thickness, it can be seen in Figure 7 that the UALC slightly drops for smaller flange thicknesses (-10% oversize) as the radius increases, stays the same for no oversize (0%), and increases for thicker flanges (+10% oversize).
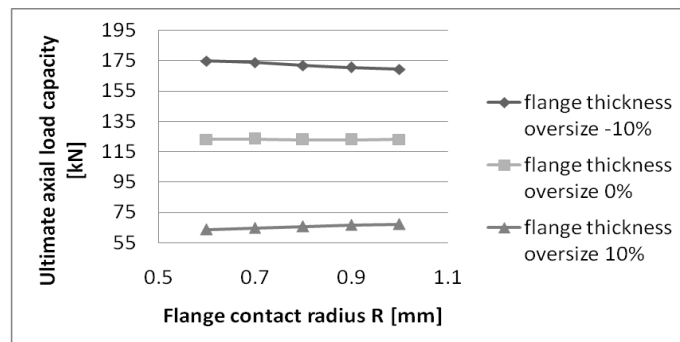


**Figure 7: UALC over the flange contact radius R, for a flange thickness oversize of -10%, 0% and 10% and an angle of 20°**

For a contact radius R of 0.6 mm, and several different flange thicknesses $t_f$, the graphs in Figure 8 show a minor dependency of the UALC on the flange angle γ. For all three thicknesses with oversize from 10% to -10%, the UALC drops as the flange angle γ increases. For these analyses only the flange angle changed but the angle of the band clamps V-section remained at 20°. This minor drop is due to the flange angle getting larger and hence the contact point moving away from the back of the section towards the flange legs. This again increases the lever and leads to less force being necessary to deform the band section.
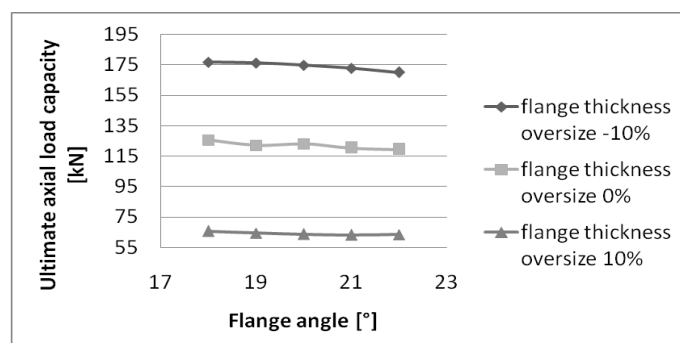


**Figure 8: Predicted UALC over the flange angle γ, for a flange contact radius R=0.6mm and varying flange thickness oversize**

Initial experimental validation of the finite element analysis methodology was obtained by investigating models with a flange diameter $D_f$ of 112 mm. The results of the finite element analyses are shown in Figure 9 and show the same tendency as band clamps with a diameter $D_f$ of 235 mm in Figure 10. Previous experimental work by Muller [15] produced the UALC values shown in Figure 10. Whilst there is significant scatter in the experimental results and the precise band geometry was not controlled, the results are within the range predicted by the finite element analysis (for $D_f$=112 mm).
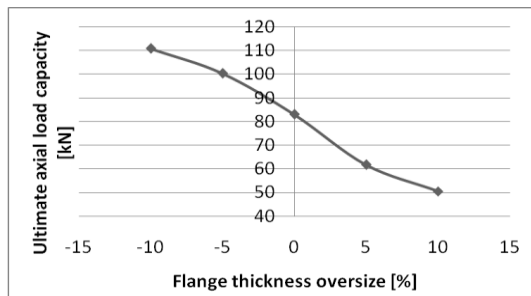
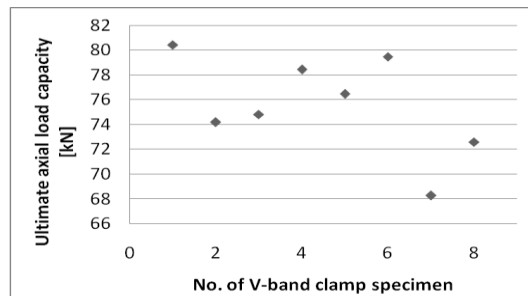**Figure 9: Predicted UALC over the flange thickness oversize, for a contact radius of R=0.8mm and an angle of 20°**



**Figure 10: Determined UALC over specimens used in experimental tests on a tensile machine, Df=112mm**

## 4    CONCLUSION AND FURTHER WORK

In this paper the influence of a number of geometrical parameters of flanges on the ultimate axial load capacity (UALC) of a V-band joint has been investigated. Using finite element analysis it was found that the thickness of the flange has the greatest influence and significantly reduces UALC as the flange gets thicker. The flange angle and contact radius only play a minor role in changing the UALC of a V-band joint.

Further work should now focus on investigating the influence of the geometrical parameters of the V-band clamp itself to the UALC. It was also noted that failure of the V-band joint was due to two effects: extension of the overall band circumference and bending of the band cross section. Further work should therefore be extended over a wide range of flange diameters to investigate the influence of these modes of failure. Additional experimental validation of the finite element work should also be established by testing bands with a range of diameters and measured geometry.

Moreover this numerical work assumed axisymmteric deformation and stresses in the V-band clamp, but in real applying deformation and stresses in the circumference do not distribute uniformly. Further work should focus on replacing the 2 dimensional model with a 3 dimensional, and investigate deformation and stresses in the circumference.

### REFERENCES

1.      Barrans, S.M. and M. Muller, *Finite element prediction of the ultimate axial load capacity of V-section band clamps*, in *7th International Conference on Modern Practice in Stress and Vibration Analysis*. 2009: Cambridge.
2.      Shoghi, K., S.M. Barrans, and H.V. Rao. *Stress in V-section band clamps*. in *Proceedings of the Institution of Mechanical Engineers*. 2004.
3.      Shoghi, K., S.M. Barrans, and H.V. Rao, *Classical and finite element analysis of V-band retainers*, in *NAFEMS World Congress*. 2003: (Orlando) Florida.
4.      Shoghi, K., S.M. Barrans, and P. Ramasamy. *Axial load capacity of V-section band clamp joints*. in *8th International Conference on Turbochargers and Turbocharging* 2006. London.
5.      Dassault-Systems, *Getting Started with ABAQUS v6.7 Section 12 Contact.* 2007.
6.      Konter, A. *How to undertake a Contact and Friction Analysis*. in *NAFEMS*. 2000. Glasgow.
7.      Dassault-Systems, *Getting Started with ABAQUS v6.7 Section 4 Using Continuum Elements.* 2007.
8.      Konter, A., *Advanced Finite Element Contact Benchmarks*, in *NAFEMS*. 2005: Glasgow.
9.      Dassault-Systems, *Getting Started with ABAQUS v6.7 Section 3.* 2007.
10.     Shoghi, K., *Stress and Strain Analysis of flat and V-section band clamps*. 2003, University of Huddersfield: Huddersfield.
11.     Dixit, P.M. and U.S. Dixit, *Modeling of Metal Forming and Machining Processes by Finite Element and Soft Computing Methods*. 2008, London: Springer. p 101.
12.     Meyers, M.A. and K.K. Chawla, *Mechanical Behavior of Materials*. 1999, London: Prentice-Hall International (UK) Ltd.
13.     Tehrani, M.S., et al., *Localised edge buckling in cold roll-forming of symmetric channel section.* Thin-walled structures, 2006. **44**: p. 184-196.
14.     Brown, I. 11-05-2009, Teconnex Ltd.: Keighley.
15.     Muller, M., *Ultimate Tensile Strength of V-Band Connectors*, in *School of Computing and Engineering*. 2007, University of Huddersfield: Huddersfield.